Raman intensities of lattice modes and the oriented gas model

E. Burgos, H. Bonadeo, and E. D'Allesio

Citation: The Journal of Chemical Physics **63**, 38 (1975); doi: 10.1063/1.431114
View online: https://doi.org/10.1063/1.431114
View Table of Contents: http://aip.scitation.org/toc/jcp/63/1
Published by the American Institute of Physics

PHYSICS TODAY
WHITEPAPERS

ADVANCED LIGHT CURE ADHESIVES

Take a closer look at what these environmentally friendly adhesive systems can do

READ NOW

PRESENTED BY
MASTERBOND
ADHESIVES | SEALANTS | COATINGS

Raman intensities of lattice modes and the oriented gas model

E. Burgos

Facultad de Ciencias Exactas y Naturales, Universidad Nacional de Buenos Aires, Buenos Aires, Argentina

H. Bonadeo* and E. D'Alessio*

Area de Investigación, Desarrollo y Servicios, Comisión Nacional de Energía Atómica, Buenos Aires, Argentina
(Received 25 November 1974)

The applicability of the oriented gas model to the calculation of Raman intensities of molecular crystals is investigated. The basic implications of the model and its consequences are discussed. The polarized spectra of only 3 out of 11 crystals considered are compatible with the model. For these, quantitative calculations based on calculated eigenvectors give reasonable agreement with experiment, while the others are in clear disagreement with available data. It is shown that assignments of unpolarized spectra based on the model's predictions may easily be erroneous. Some of the parameters affecting the calculation are analyzed, confirming the conclusion that the oriented gas model is not a reliable tool for assignment of Raman lattice bands of molecular crystals.

INTRODUCTION

Raman bands due to lattice vibrations are unequivocally assigned to their proper factor group species by recording polarized spectra of single crystals. These spectra, however, are not always available for molecular crystals, since a large number of them offer considerable experimental difficulties. In these cases, additional theoretical considerations might be of great use. For internal modes, comparison of observed relative intensities and those calculated using the oriented gas model give good qualitative agreement.[1-3] For external modes, however, this calculation has been mostly limited by the lack of knowledge of the actual crystal normal modes, and additional approximations assuming uncoupled rotations about molecular principal axes have led to unsatisfactory results.[4] Recently, Elliot and Leroi have used the model in combination with lattice dynamical calculation to assign the unpolarized spectra of benzene[5] and ethylene,[6] using the results for the latter as an important argument to decide on its crystal structure.

In the last few years, several different intermolecular force field models of the atom–atom type have been developed to fit simultaneously statical and dynamical properties of molecular crystals.[7,8] The resulting calculated crystal vibration frequencies have contributed to the assignment of some normal modes and, in addition, provide a quantitative description for external modes in terms of rotation and translation coordinates. As these coordinates are used as a basis for constructing the dynamical matrix, the eigenvectors of the secular equation give a direct description of how the mixing of molecular librations and translations gives rise to an external crystal normal mode. Nevertheless, these calculations, although adequate, may contain inversions regarding the frequency ordering of some normal modes of different symmetry, thus limiting their capacity to define assignments in unpolarized spectra.

In the present work, we explore the possibilities offered by the applications of the oriented gas model in combination with lattice mode frequency calculations to predict Raman band intensities and positions, in order to contribute to the assignment of external modes.

It must be stressed that owing to the uncertainties in experimental intensities, and to the roughness of the oriented gas model, only qualitative agreement could be expected. However, knowledge of relative orders of magnitude should be of great use, allowing, for instance, the prediction of vanishingly low observable intensities.

We have applied the model to a series of 11 molecular crystals including aromatic hydrocarbons and chlorinated and brominated benzenes. For these compounds, the crystal structure is known and a large number of low frequency Raman bands has been observed and assigned, making a qualitative discussion possible. On the other hand, except for the brominated benzenes, intermolecular force fields are available, allowing also a quantitative test of the model.

CALCULATION METHOD

The relative intensities in polarized and unpolarized Raman spectra for a nondegenerate normal mode Q_n can be calculated by

$$I_{\rho\sigma}(Q_n) = \frac{\text{const}}{\nu_n[1-\exp(-h\nu_n/kT)]} \left| \frac{\partial(\alpha_u)_{\rho\sigma}}{\partial Q_n} \right|^2 ,$$
$$I(Q_n) = \sum_\rho \sum_\sigma I_{\rho\sigma}(Q_n) , \tag{1}$$

respectively. ρ and σ label coordinates of an orthogonal set of coordinates fixed to the crystal, ν_n is the frequency of the normal mode, and $(\alpha_u)_{\rho\sigma}$ is the $\rho\sigma$th element of the unit cell polarizability tensor. When crystal modes are expressed in terms of some set of molecular coordinates, the derivatives of the molecular polarizabilities can be written as

$$\frac{\partial(\alpha_u)_{\rho\sigma}}{\partial Q_n} = \sum_m \sum_k \frac{\partial(\alpha_u)_{\rho\sigma}}{\partial q_{km}} \frac{\partial q_{km}}{\partial Q_n} , \tag{2}$$

where q_{km} is the kth coordinate of the set chosen for the mth molecule in the unit cell.

The oriented gas model that is used in the present calculation is based on the following hypotheses:

(a) the molecular polarizabilities are additive;

(b) the charge distribution in each molecule is deter-

 Copyright © 1975 American Institute of Physics

TABLE I. Relative intensities compatible with the model in three orthogonal polarizations.

I_1	$\geq$	I_2	$\geq$	I_3
100		100		0
100		81		1
100		64		4
100		49		9
100		36		16
100		25		25

mined by the intramolecular field only and is consequently independent of motions and distortions introduced by other molecules of the crystal.

Statement (b) is equivalent to saying that the molecular polarizability does not change while the molecule translates or librates. According to (a), the crystal polarizability tensor α_u is related to the molecular polarizability α by

$$\alpha_u = \sum_m \pi_m \alpha \tilde{\pi}_m , \tag{3}$$

where π_m is the matrix relating molecular principal axes corresponding to the mth molecule and the crystal fixed axes.

The derivatives of α_u with respect to principal molecular axes rotation and translation coordinates R_{km} and T_{km} can be calculated, according to (b), as

$$\frac{\partial \alpha_u}{\partial R_{km}} = \pi_m(\mathbf{M}_k\alpha + \alpha\tilde{\mathbf{M}}_k)\tilde{\pi}_m ,$$
$$\frac{\partial \alpha_u}{\partial T_{km}} = 0 , \tag{4}$$

with $(\mathbf{M}_k)_{ij} = -\epsilon_{ijk}$, the Levi–Civita tensor. It can be seen that translations do not contribute, in this model, to Raman intensities.

The rotation coordinates R_{km} can be expressed in terms of symmetry coordinates $S_k(\gamma)$. The derivatives of the element $(\alpha_u)_{\rho\sigma}$ with respect to external normal coordinates $Q_n(\gamma)$ of symmetry γ are obtained by

$$\frac{\partial(\alpha_u)_{\rho\sigma}}{\partial Q_n(\gamma)} = \sum_m \sum_k \frac{\partial R_{km}}{\partial S_k(\gamma)} \frac{\partial S_k(\gamma)}{\partial Q_n(\gamma)} [\pi_m(\mathbf{M}_k\alpha + \alpha\tilde{\mathbf{M}}_k)\tilde{\pi}_m]_{\rho\sigma} . \tag{5}$$

If the polarizability and inertia principal axes do coincide, this expression can be simplified:

$$\frac{\partial(\alpha_u)_{\rho\sigma}}{\partial Q_n(\gamma)} = \sum_m \sum_k \frac{\partial R_{km}}{\partial S_k(\gamma)} \frac{\partial S_k(\gamma)}{\partial Q_n(\gamma)} (\alpha_{k+1,k+1} - \alpha_{k+2,k+2}) \times [(\pi_m)_{\rho,k+1}(\pi_m)_{\sigma,k+2} + (\pi_m)_{\rho,k+2}(\pi_m)_{\sigma,k+1}] .$$

In these equations, the derivatives $\partial R_{km}/\partial S_k(\gamma)$ and the transformation matrices π_m are obtained from crystal data, and the α tensor is the polarizability expressed in principal axes. If the molecular distortion is not very important, free molecule polarizabilities can be used. The derivatives $\partial S_k(\gamma)/\partial Q_n(\gamma)$ which express the composition of each crystal mode are determined from the eigenvectors of the dynamical matrix diagonalization.

APPLICATION OF THE ORIENTED GAS MODEL TO EXTERNAL MODES

Intermolecular and intramolecular force fields are involved in the calculation of Raman intensities by the oriented gas model. Nevertheless, this model makes a clear distinction between both fields when it considers that the molecular polarizabilities produced by the internal field are unchanged when the crystal field acts on the molecules during the vibrational motion. This assumption implies that the trace of the polarizability tensor, which is invariant with respect to similarity transformations, is preserved during librations in any orthogonal coordinate system and therefore

$$\frac{\partial(\alpha_m)_{xx}}{\partial Q_n} + \frac{\partial(\alpha_m)_{yy}}{\partial Q_n} + \frac{\partial(\alpha_m)_{zz}}{\partial Q_n} = 0 \tag{6}$$

for the mth molecule in the nth normal mode Q_n. From the additivity hypothesis, it is possible to extend expression (6) to the crystal unit cell:

$$\frac{\partial(\alpha_u)_{xx}}{\partial Q_n} + \frac{\partial(\alpha_u)_{yy}}{\partial Q_n} + \frac{\partial(\alpha_u)_{zz}}{\partial Q_n} = 0 . \tag{7}$$

It must be stressed that this relationship stems from the basic assumption of the model only and is independent from other factors of the intensity calculation such as crystal structure, polarizabilities, and eigenvectors of the secular equation.

Equation (7) establishes relationships between permissible relative intensities in three orthogonal polarizations $\rho\rho$, $\sigma\sigma$, and $\tau\tau$ with $\rho \perp \sigma \perp \tau$, which can be summarized by

$$4I_2 \geq I_1 \geq 4I_3 ,$$
$$2(I_2 + I_3) \geq I_1 \geq (I_2 + I_3) \tag{8}$$

for $I_1 \geq I_2 \geq I_3$. (See Table I).

Even though other invariants of the polarizability tensor do not provide direct relationships between observables, Eq. (8) constitutes a rough guideline for the applicability of the model.

Raman intensities are in general poorly determined experimental data. In particular, intensities in three orthogonal polarizations cannot be compared directly owing to unavoidable modifications in the experimental setup. However, both the guideline expressed in Eq. (8) and the results from more refined calculations can be applied admitting a possible correction factor common to all bands observed in each polarization. The magnitude of this factor may be estimated within the assumptions of the model. In general, owing to the orthogonality of normal modes,

$$C_{\rho\sigma} = \text{const} \sum_n \nu_n [1 - \exp(-h\nu_n/kT)] I_{\rho\sigma}(Q_n)$$
$$= \text{const} \sum_m \sum_k \left| \frac{\partial(\alpha_u)_{\rho\sigma}}{\partial q_{km}} \right|^2 \tag{9}$$

The observable relation $C_{\rho\sigma}/C_{\rho'\sigma'}$ is independent from the mixing of librations in the normal modes and q_{km} in (9) can be replaced by R_{km}. The oriented gas model can only predict spectra compatible with values of $C_{\rho\sigma}$ calculated according to (9) together with relative intensities restricted by (8).

TABLE II. Compatibility of the oriented gas model with observed polarized spectra.

	Restrictions of the model		
Crystal	Intensity relations in three orthogonal polarizations ($I_{aa}:I_{bb}:I_{cc}$)	Ability to predict zero intensity bands	Compatibility with $C_{\rho\sigma}/C_{\rho'\sigma'}$
Naphthalene[a]	yes	yes	yes
Anthracene[a]	yes	yes	yes
Biphenyl[a]	yes[g]	yes[g]	yes
Benzene[b]	yes	yes	no
β-p-dichlorobenzene[a]	yes	no	yes
p-dibromobenzene[a]	yes	no	yes
1,3,5-trichlorobenzene[c]	no	yes	no
1,3,5-tribromobenzene[d]	no	yes	no
1,2,4,5-tetrachlorobenzene[e]	no	yes	no
Hexachlorobenzene[f]	...	yes	yes

[a]Spectra from Ref. 4.
[b]Spectra from Ref. 12.
[c]Spectra from Ref. 13, 14.
[d]Spectra from Ref. 13.
[e]Spectra from Ref. 15.
[f]Spectra from Ref. 16. Incomplete polarization data.
[g]If there are two nonresolved Ag bands.

Finally, we can analyze the possibilities of the model considering that for each symmetry species the symmetry coordinates $S_k(\gamma)$ form a basis for the corresponding vector space. The derivatives

$$\frac{\partial(\alpha_u)_{\rho\sigma}}{\partial Q_n(\gamma)} = \sum_k \frac{\partial(\alpha_u)_{\rho\sigma}}{\partial S_k(\gamma)} \frac{\partial S_k(\gamma)}{\partial Q_n(\gamma)} = \sum_k [F_{\rho\sigma}(\gamma)]_k \frac{\partial Q_n(\gamma)}{\partial S_k(\gamma)}$$

with

$$[F_{\rho\sigma}(\gamma)]_k = \frac{\partial(\alpha_u)_{\rho\sigma}}{\partial S_k(\gamma)} \tag{10}$$

may be viewed as the scalar product $\bar{Q}_n(\gamma)\cdot\bar{F}_{\rho\sigma}(\gamma)$, the intensities $I_{\rho\sigma}$ being proportional to the square of the projections of $\bar{F}_{\rho\sigma}(\gamma)$ onto $\bar{Q}_n(\gamma)$ considered as a vector in the symmetry space γ. The absolute value of $\bar{F}_{\rho\sigma}(\gamma)$ is

$$|\bar{F}_{\rho\sigma}(\gamma)| = \begin{cases} \text{const}\, C_{\rho\sigma}, & \text{if } (\alpha_u)_{\rho\sigma} \in \gamma \\ 0, & \text{otherwise.} \end{cases} \tag{11}$$

For rigid body external motions, the six nonvanishing $\bar{F}_{\rho\sigma}(\gamma)$ vectors are determined, within the assumptions of the model, by molecular polarizabilities and crystal structures only. Even though the space is hexadimensional, for noncentrosymmetric molecular sites, the components of $\bar{F}_{\rho\sigma}(\gamma)$ vanish for the three translational coordinates according to Eq. (4). In general, this description establishes that the maximum number of zero intensity modes $Q_n(\gamma)$ predicted by the model for each symmetry species γ is equal to the difference between the dimensions of the γ symmetry space and the subspace spanned by the nonvanishing $\bar{F}_{\rho\sigma}(\gamma)$ vectors. In this sense, the invariance of the trace [Eq. (7)], and the definition in Eq. (10), show that

$$\sum_{\rho=1}^{3} \bar{F}_{\rho\rho}(\gamma) = 0,$$

and thus, these vectors are coplanar and the model accepts that a mode $\bar{Q}_n(\gamma) \sim \bar{F}_{\rho\rho}(\gamma) \times \bar{F}_{\sigma\sigma}(\gamma)$, $\rho \neq \sigma$, may have zero intensity in three orthogonal polarizations even though it is Raman active by symmetry.

We can take, for example, the space group C_{2h}^5 with two molecules per unit cell located at C_i sites, which is a very common case for molecular crystals.[9] The symmetry space γ is tridimensional. For Bg modes, as only $\bar{F}_{ab}$ and $\bar{F}_{bc}$ are nonzero, except for accidental degeneracies, only one mode may have zero intensity. As $\bar{F}_{ac}(Ag)$ does not lie in the same plane as $\bar{F}_{\rho\rho}(Ag)$, the model does not allow zero intensity Ag bands. The accidental degeneracies may stem from molecular or crystal structure. If the molecular polarizability tensor is diagonal [reduced form of Eq. (5)] and has two identical elements, all vectors $\bar{F}_{\rho\sigma}(\gamma)$ have to lie in the degenerate plane. If the crystal unique axis coincides with a molecular principal axis, all $\bar{F}_{\rho\sigma}(Ag)$ are parallel to this axis, and there may be up to two Ag zero intensity modes.

CRYSTAL NORMAL MODE CALCULATION

The calculation method used in the present work is discussed in detail in Ref. 10. We have used an atom–atom intermolecular potential of the form

$$V_{ij} = -Ar_{ij}^{-6} + B\exp(-Cr_{ij}).$$

The eigenvectors provide a direct picture of the degree of mixing of molecular rotations and translations in each normal mode. For the case of benzene, they were taken directly from Ref. 10. In all cases, atom–atom contacts up to a distance of 6 Å were taken into account. The rigid body approximation has been used throughout, as it is a negligible source of errors for the eigenvectors.[11]

RESULTS AND DISCUSSION

First we will discuss the applicability of the model to a series of Raman spectra of molecular crystals in semiqualitative terms. Table II summarizes the compatibility of the observed spectra with three main features of the model which do not depend on the intermolecular force field.

For naphthalene and anthracene, the intensity relations for the three Ag modes and the values of $C_{\rho\rho}$ in three orthogonal polarizations are acceptable, and all three allowed bands are observed. Values of $C_{\rho\sigma}$ ($\rho \neq \sigma$) are also consistent, and the model would be *a priori* applicable.

For benzene, although the Ag band intensities relation is preserved, the value of C_{ac}, predicting a very weak spectrum in that polarization, is in contradiction with experiment.

For biphenyl, the band at 54 cm^{-1} escapes the scheme of Table I. As no structural near-degeneracy occurs, the absence of one Ag band cannot be accounted for by the model, except if one postulates two nonresolved Ag bands, as the calculation suggests.[17] This also happens for the β-p-dichlorobenzene and p-dibromobenzene crystals, where only two Ag bands have been observed.

For 1, 3, 5-trichlorobenzene and 1, 3, 5-tribromoben-

TABLE III. Observed and calculated frequencies, normal mode composition, and calculated relative intensities for crystals under consideration.

				Normal modes			Relative intensities[k]						
Crystal	Sym.	ν_{expt} (cm^{-1})	ν_{calc} (cm^{-1})	*Rx*	*Ry*	*Rz*	*aa*	*bb*	*cc*	*ac*	*ab*	*bc*	Total
		84	76.8	0.15	−0.01	−0.99							6
α-*p*-$C_6H_4Cl_2$[a]		56	54.2	0.88	0.45	0.13							34
		45	41.7	0.45	−0.89	0.08							100
		103	110.4	−0.15	−0.11	−0.98	0	3	2	1			7
	Ag	65	63.4	0.71	−0.70	−0.03	10	0	14	12			49
β-*p*-$C_6H_4Cl_2$[b]		...	49.7	−0.69	−0.70	0.18	14	39	6	20			100
		108	115.3	−0.02	−0.35	−0.94					0	2	3
	Bg	55	59.9	−0.98	−0.17	0.08					1	2	6
		31	35.2	−0.18	0.92	−0.34					21	18	77
	$C_{\rho\sigma}$[j]						60	100	67	79	23	38	
		58	61.4	−0.90	−0.23	−0.36	2	1	1	0			4
	Ag	46	54.8	0.42	−0.32	−0.85	2	1	4	3			12
		36	35.5	0.08	−0.92	0.39	4	4	0	6			19
1,2,4,5-$C_6H_2Cl_4$[c]		...	69.1	0.00	0.08	0.99					1	1	3
	Bg	49	47.6	0.98	0.19	−0.01					0	0	0
		21	18.5	0.19	−0.98	0.08					2	48	100
	$C_{\rho\sigma}$						82	38	65	73	17	100	
		56	52.4	−0.75	−0.64	0.14	6	3	0	0			10
	Ag	45	39.9	0.44	−0.65	−0.62	18	24	1	3			49
		21	28.1	−0.49	0.40	−0.77	2	1	5	10			28
C_6Cl_6[d]		54	51.0	−0.47	−0.88	0.10					15	6	42
	Bg	38	38.3	0.43	−0.33	−0.84					9	24	67
		25	26.2	−0.77	0.35	−0.54					4	46	100
	$C_{\rho\sigma}$						54	59	7	16	67	100	
		57	53.7	0.09	−0.16	−0.05	1	0	1				2
		...	45.5	0.79	−0.24	−0.04	3	0	3				6
	A_1	46	43.7	0.31	0.93	0.14	45	0	49				94
		34	34.0	−0.16	0.17	−0.79	5	3	1				8
		30	28.5	0.44	−0.14	−0.01	2	0	3				5
		23	20.0	−0.23	−0.02	0.59	1	4	1				6
		61	58.6	−0.18	0.93	0.18						2	3
		54	47.0	−0.72	0.03	0.06						0	0
	B_1	46	45.0	0.38	−0.01	0.85						50	100
		34	33.9	−0.55	−0.36	0.46						24	49
1,3,5-$C_6H_3Cl_3$[d]		...	30.0	0.07	−0.01	0.13						3	5
		56	55.2	−0.11	0.91	0.09				19			38
		44	42.7	0.08	0.22	−0.11				2			4
	B_2	...	36.8	0.64	0.18	0.57				0			1
		32	32.8	−0.52	0.24	−0.16				4			9
		22	22.2	−0.55	0.16	0.79				0			0
		58	54.8	−0.21	0.37	−0.08					0		0
		...	51.5	0.55	0.69	0.29					2		5
	B_3	48	45.3	−0.37	0.32	0.61					7		14
		36	41.2	0.15	0.42	−0.70					6		13
		31	31.1	0.71	−0.34	0.22					1		1
	$C_{\rho\sigma}$						74	3	77	50	23	100	
		92	95.0	−0.64	0.47	−0.60	40	2	25				67
	Ag	79	75.0	−0.58	−0.81	−0.01	3	20	37				59
		57	55.0	−0.50	0.34	−0.80	59	2	39				100
		128	128.0	−0.94	0.30	0.15						2	5
	B_{1g}	100	96.0	−0.26	−0.94	0.22						23	46
C_6H_6[f]		(57)	60.0	0.21	0.17	0.96						1	3

TABLE III *(Continued)*

Crystal	Sym.	ν_{expt} (cm^{-1})	ν_{calc} (cm^{-1})	Normal modes Rx	Ry	Rz	Relative intensities[k] aa	bb	cc	ac	ab	bc	Total
C_6H_6[f]		...	101.0	−0.39	0.92	0.09				3			5
	B_{2g}	90	93.0	−0.34	−0.23	0.91				0			1
		79	83.0	0.86	0.32	0.40				1			2
		128	127.0	−0.96	0.27	0.03					1		2
	B_{3g}	(92)	89.0	−0.16	−0.46	−0.87					7		14
		61	66.0	−0.22	−0.85	0.48					36		72
	$c_{\rho\sigma}$						100	24	100	6	41	42	
		109	104.9	−0.84	−0.53	0.12	23	16	1	0			40
	Ag	74	75.7	0.53	−0.85	−0.06	10	2	22	33			100
		51	51.5	0.13	0.02	0.99	0	3	2	0			5
$C_{10}H_8$[g]		125	101.1	−0.99	−0.09	−0.07					10	1	21
	Bg	71	70.6	0.10	−0.96	−0.26					1	16	33
		46	45.4	0.04	0.27	−0.96					1	0	3
	$c_{\rho\sigma}$						100	62	46	64	34	30	
		121	116.3	0.95	0.22	−0.23	6	4	0	0			10
	Ag	70	72.9	0.25	−0.96	0.10	32	0	33	18			100
		39	38.9	−0.20	−0.15	−0.97	0	8	6	0			15
$C_{14}H_{10}$[h]		125	107.7	−0.99	−0.08	0.05					3	1	7
	Bg	65	64.7	0.07	−0.99	−0.14					2	17	38
		45	47.4	0.06	−0.13	0.99					5	12	35
	$c_{\rho\sigma}$						100	26	76	39	22	43	
		88	80.9	0.41	−0.06	0.91	11	12	0	1			24
	Ag	54	56.6	0.68	0.68	−0.26	7	2	16	38			100
		...	51.5	0.61	−0.73	−0.32	20	5	5	13			55
$C_{12}H_{10}$[i]		88	82.0	−0.37	−0.84	0.40					1	5	12
	Bg	54	65.3	0.15	0.38	0.91					2	3	9
		42	42.9	0.92	−0.40	0.02					4	41	90
	$c_{\rho\sigma}$						92	58	41	100	14	77	

[a]Frequencies at 300 K, our measurement. Crystal structure at 300 K, Ref. 18. $\alpha_{xx}=9.4$; $\alpha_{yy}=13.1$; $\alpha_{zz}=18.6$ (Å^3), Ref. 19. $I_{xx}>I_{yy}>I_{zz}$.

[b]Frequencies interpolated at 138 K, according to Refs. 4 and 20. Crystal structure at 138 K, Ref. 18. Molecular polarizabilities from Ref. 19. $I_{xx}>I_{yy}>I_{zz}$.

[c]Frequencies at 300 K, Ref. 15. Crystal structure at 300 K, Ref. 21. $\alpha_{xx}=12.3$; $\alpha_{yy}=19.7$; $\alpha_{zz}=22.4$ (Å^3), estimated by the authors. $I_{xx}>I_{yy}>I_{zz}$.

[d]Frequencies at 300 K, Ref. 16. Crystal structure at 300 K, Ref. 18. $I_{xx}>I_{yy}\simeq I_{zz}$.

[e]Frequencies at 300 K, Ref. 14. Crystal structure at 300 K, Ref. 18. $I_{xx}>I_{yy}\simeq I_{zz}$. Only the librational components of eigenvectors are tabulated.

[f]Frequencies at 140 K, Ref. 12. Calculated frequencies and mode composition from Ref. 10. $I_{zz}>I_{yy}\simeq I_{xx}$.

[g]Frequencies at 300 K, Refs. 4 and 22. Crystal structure at 300 K, Ref. 23. $\alpha_{xx}=20.2$; $\alpha_{yy}=18.8$; $\alpha_{zz}=10.7$ (Å^3). $I_{zz}>I_{yy}>I_{xx}$, Ref. 19.

[h]Frequencies at 300 K, Refs. 4 and 22. Crystal structure at 300 K, Ref. 24. $\alpha_{xx}=35.2$; $\alpha_{yy}=25.6$; $\alpha_{zz}=15.2$ (Å^3). $I_{zz}>I_{yy}>I_{xx}$, Ref. 19.

[i]Frequencies at 300 K, Ref. 4. Crystal structure at 300 K, Ref. 25. $\alpha_{xx}=13.84$; $\alpha_{yy}=20.28$; $\alpha_{zz}=24.74$ (Å^3). $I_{xx}>I_{yy}>I_{zz}$, Ref. 26.

[j]Tabulated values normalized to 100 for the largest $C_{\rho\sigma}$.

[k]Tabulated values normalized to 100 for the largest intensity in unpolarized spectrum for each crystal.

zene, the bands at 57 cm^{-1} and 48 cm^{-1}, respectively, are observed only with *bb* polarization, and therefore incompatible with the model. In the case of 1, 2, 4, 5-tetrachlorobenzene, the intensity relations for *Ag* modes is in doubtful agreement with the model. Also, the magnitude of disagreement between observed and calculated values of $C_{\rho\sigma}$ for these crystals cannot be attributed to change in experimental setups only.

For α-*p*-dichlorobenzene, there are no polarized spectra, while for hexachlorobenzene the data are incomplete. For this last crystal, the model seems to be appropriate.

Even though the qualitative agreement is not particularly encouraging, we have performed quantitative calculations for the crystals under consideration (except for the

TABLE IV. Relative intensities for β-p-dichlorobenzene obtained for three different sets of molecular polarizabilities.

Sym.	ν_{calc}	Molecular polarizabilities	aa	bb	cc	ac	ab	bc	Total
		a	0	3	2	1			7
	110.4	b	0	2	1	0			4
		c	0	7	6	3			19
		a	10	0	14	12			49
Ag	63.4	b	13	0	14	11			48
		c	4	4	16	14			52
		a	14	39	6	20			100
	49.7	b	18	43	5	17			100
		c	6	28	8	29			100
		a					0	2	3
	115.3	b					0	1	2
		c					0	4	8
		a					1	2	6
Bg	59.9	b					1	3	8
		c					1	1	3
		a					21	18	77
	35.2	b					17	18	71
		c					31	16	93

[a] $\alpha_{xx}=9.4$; $\alpha_{yy}=13.1$; $\alpha_{zz}=18.6$ (Å^3), Ref. 19.
[b] $\alpha_{xx}=8.83$; $\alpha_{yy}=12.48$; $\alpha_{zz}=21.29$ (Å^3), Ref. 27.
[c] $\alpha_{xx}=9.36$; $\alpha_{yy}=15.12$; $\alpha_{zz}=18.02$ (Å^3), Ref. 28.

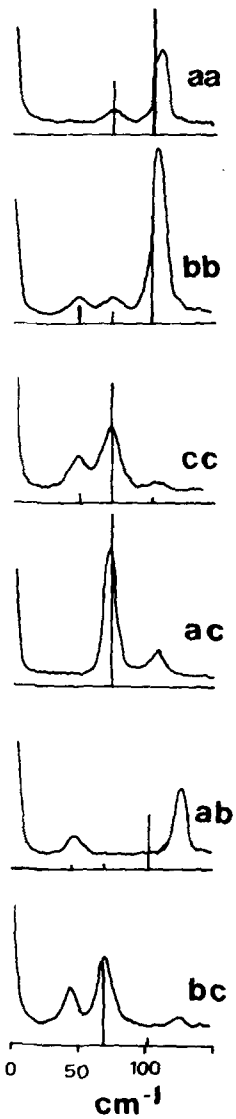

FIG. 1. Polarized Raman spectrum of naphthalene, Ref. 4. Calculated frequencies and relative intensities are represented by full lines.

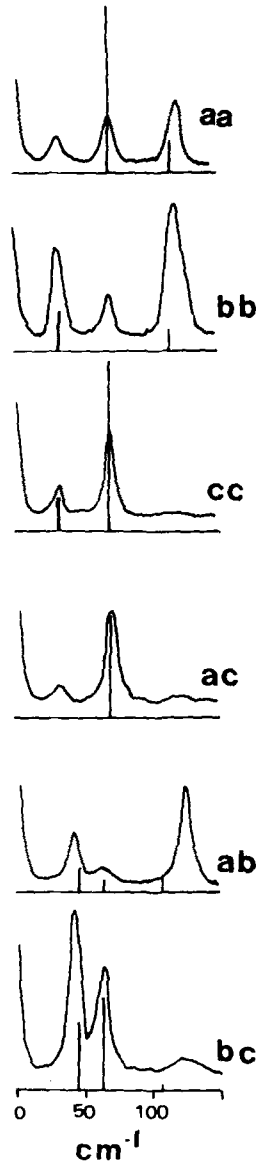

FIG. 2. Polarized Raman spectra of anthracene, Ref. 4. Calculated frequencies and relative intensities are represented by full lines.

brominated benzenes, for which no suitable potential parameters are available) in order to see if some general features of the spectra could be deduced from the application of the model.

For the hydrocarbons we have used atom–atom potential parameters proposed by Williams,[7] and for chlorinated benzenes, those obtained by Bonadeo and D'Alessio.[11]

The transformation matrices relating molecular principal axes and crystal fixed axes were obtained from crystal structural data. For monoclinic crystals we have chosen a crystal system ($a'bc$) with $a' \perp bc$, or (abc') with $c' \perp ab$, according to the available experimental polarizations.

In every case we have employed molecular polarizabilities from the isolated molecules without further refinements. In the same approximation, justified by the smallness of the molecular distortion in the crystal, we have assumed that the polarizability tensor is diagonal in the principal inertia axes system and applied the re-

duced expression of Eq. (5) for the calculation. Thus, the molecular polarizabilities do not appear in calculations for 1, 3, 5-trichlorobenzene, hexachlorobenzene, and benzene, where only one difference between diagonal elements is nonzero and appears as a scaling factor. In the other cases, the polarizabilities used in the calculations are included in the corresponding table.

Table III shows the calculated frequencies, intensities, and eigenvectors for each normal mode of the crystals under consideration. Figures 1–10 show the observed spectra, and, indicated by vertical lines, the calculated intensities for the bands, in arbitrary units.

The eigenvectors listed in Table III show that in most cases it is impossible to think of crystal normal modes as being pure rotations around principal molecular axes. In fact, most modes are mixed more than 20%, and only in the case of anthracene do all modes have less than 10% coupling. This result shows that, except for a few cases where the moments of inertia are widely different, the assumption of uncoupled rotations is unrealistic. On the other hand, calculated intensities may depend strongly on the eigenvectors. In anthracene, for instance, the assumption of pure rotations leads to a 46: 100 ratio for the intensities of the 121 cm^{-1} band in the *aa* and *bb* polarizations, while our calculation, with an eigenvector containing 90% rotation about the lowest moment inertia axis leads to a 148: 100 ratio. However, reasonable changes in the eigenvectors do not alter the order of magnitude of the calculated intensities.

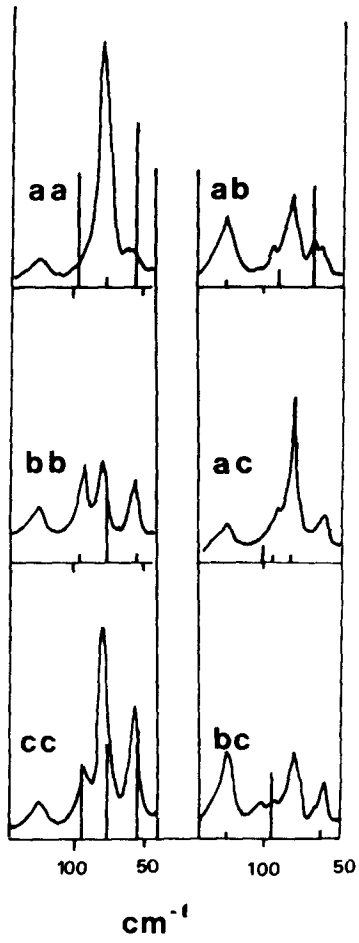

FIG. 4. Polarized Raman spectra of benzene, Ref. 12. Calculated frequencies and relative intensities are represented by full lines.

Table IV shows the results obtained for β-*p*-dichlorobenzene using three different sets of molecular polarizabilities. It can be seen that the general pattern is not substantially changed in the unpolarized spectrum, although some relative intensities may change by factors

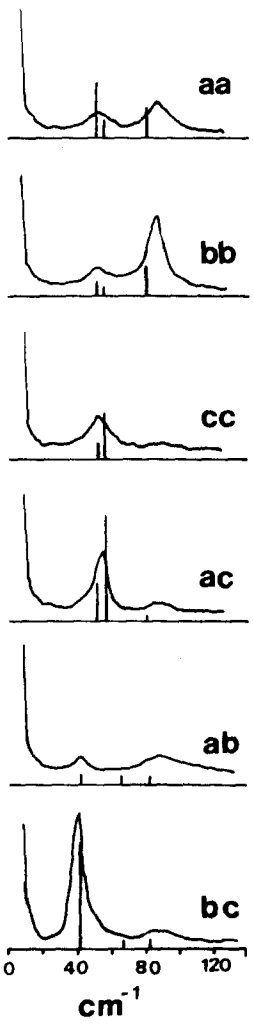

FIG. 3. Polarized Raman spectra of biphenyl, Ref. 4. Calculated frequencies and relative intensities are represented by full lines.

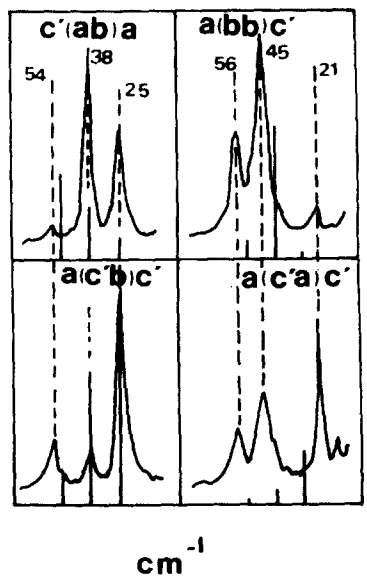

FIG. 5. Polarized Raman spectra of hexachlorobenzene, Ref. 16. Calculated frequencies and relative intensities are represented by full lines.

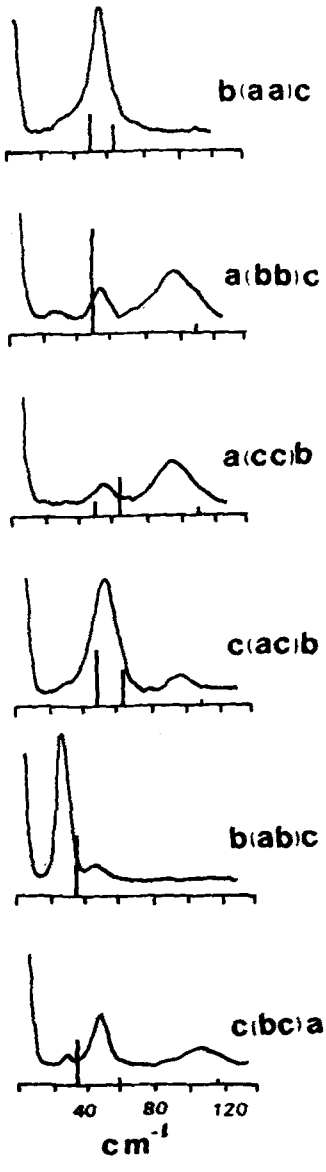

FIG. 6. Polarized Raman spectra of β-p-dichlorobenzene, at 300 K, Ref. 4. Calculated frequencies and relative intensities at 138 K are represented by full lines.

as large as 4 or 5. The differences in the polarized predictions are much larger, the intensity of some bands changing as much as 20% of the intensity of the strongest band.

As discussed before, the oriented gas model is *a priori*

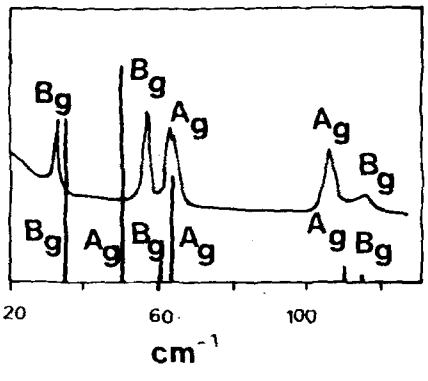

FIG. 7. Unpolarized Raman spectrum of β-p-dichlorobenzene at 108 K, Ref. 20. Calculated frequencies and relative intensities at 138 K are represented by full lines.

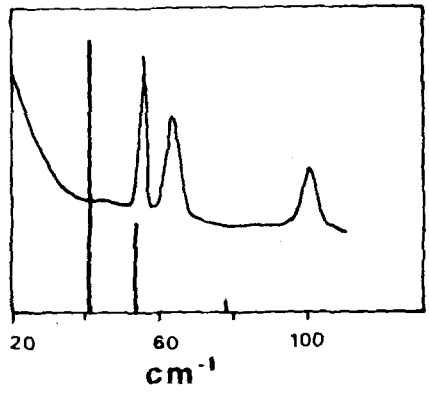

FIG. 8. Unpolarized Raman spectrum of α-p-dichlorobenzene at 108 K, Ref. 20. Calculated frequencies and relative intensities at 300 K are represented by full lines.

compatible with the polarized spectra of naphthalene and anthracene. It can be seen in Figs. 1 and 2 that the model's prediction of the intensity pattern is acceptable, within the roughness of the model and the uncertainties in the observed spectra. For biphenyl, Fig. 3, if one accepts that the band at 54 cm^{-1} is the superposition of two Ag bands, as suggested by our calculations, the results are acceptable too.

Elliot and Leroi[5] have performed an oriented gas model intensity calculation for the nonpolarized spectrum of benzene. At the time of their work, the polarized spectra were not available. Although on the basis of calculated intensities they correctly assigned the 61 cm^{-1} band to the B_{3g} species, they were led to attribute the 100 cm^{-1} band to a superposition of B_{2g} and B_{3g} modes, while the polarized spectra clearly show that it belongs to the B_{1g} species. Their calculated results do not agree with ours, maybe because we use different eigenvectors, but both predict a low intensity ac spectrum, which again does not agree with experiment (see Fig. 4).

For hexachlorobenzene, Fig. 5, the ab polarization prediction widely fails, while the rest of the pattern is halfway compatible with observed spectra.

For β-p-dichlorobenzene, Fig. 6, the superposition of two Ag bands is not supported by any theoretical or experimental argument. In any case, the polarized spectra do not agree with the model's predictions, the biggest problem being that the lowest lying Ag mode, not observed, is predicted to be the most intense band of the spectrum. Figure 7 shows an unpolarized spectrum and the corresponding calculated intensities. It can be seen that if one would rely on the calculation, the Bg band at 55 cm^{-1} would be mistakenly assigned to the Ag species. This type of results is a warning against the use of the model in the assignment of bands.

The calculated pattern agrees well with the unpolarized spectrum of α-p-dichlorobenzene, Fig. 8, but this result is not very significant since only three bands are involved.

1, 3, 5-trichlorobenzene, Fig. 9, and 1, 2, 4, 5-tetrachlorobenzene, Fig. 10, could not be expected to yield good agreement; in fact, the calculations give results which are completely contradictory with the spectra.

CONCLUSIONS

In the present work, we have considered the applicability of the oriented gas model to 11 molecular crystals. Out of these, only two (naphthalene and anthracene) undoubtedly meet the conditions imposed by the basic assumptions of the model, and biphenyl may be included in this category with additional assumptions on the interpretation of the spectra, while for hexachlorobenzene and α-*p*-dichlorobenzene the available data are incomplete. For the rest of the crystals, *a priori* considerations show that the model is inadequate.

Quantitative calculations on nine of these crystals using available force fields show that while for naphthalene, anthracene and biphenyl the model yields results which roughly agree with experiment, the predictions for the other crystals are in clear contradiction with experimental data.

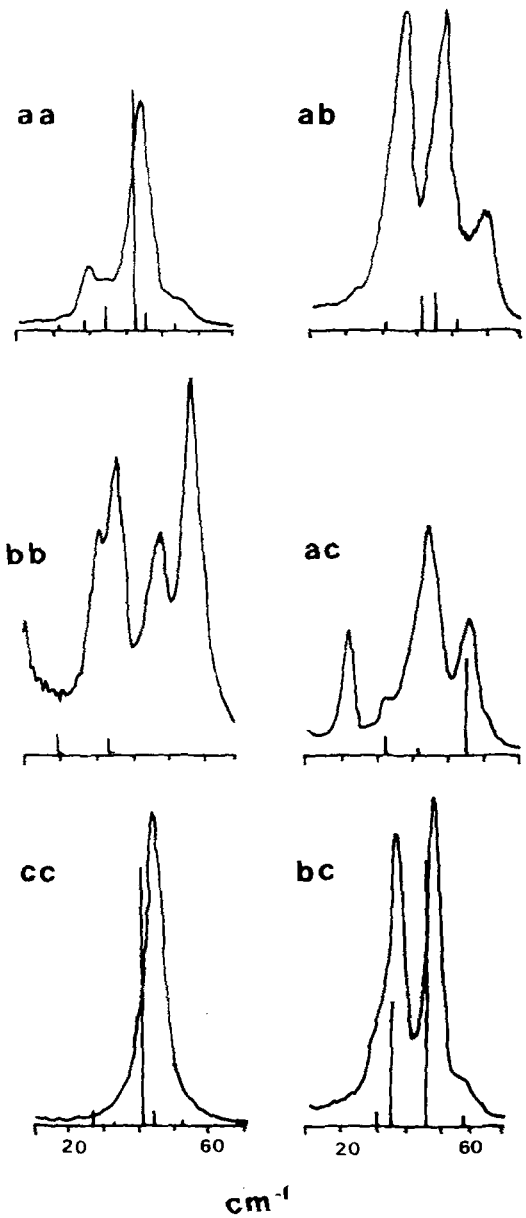

FIG. 9. Polarized Raman spectra of 1,3,5-trichlorobenzene, Ref. 16. Calculated frequencies and relative intensities are represented by full lines.

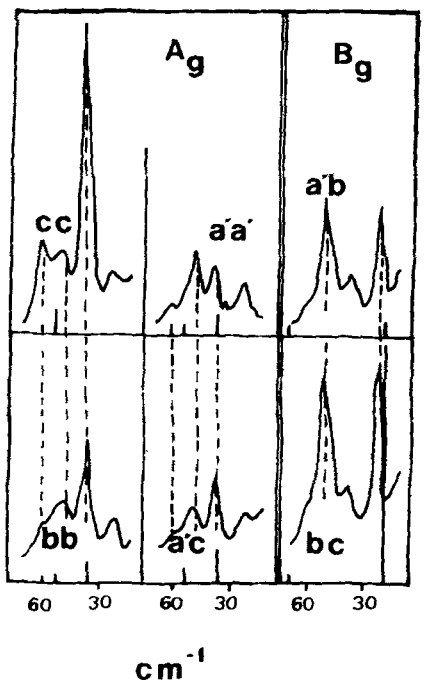

FIG. 10. Polarized Raman spectra of 1,2,4,5-tetrachlorobenzene, Ref. 15. Calculated frequencies and relative intensities are represented by full lines.

These results are rather discouraging, since the *a priori* applicability, which seems to be a good criterion by which to judge calculated intensities, is verifiable only if polarized spectra are available, in which case the assignment of the bands is experimentally assured. Therefore, the usefulness of the heuristic power of the model is severely limited: we have shown how assignments based on the model may easily be erroneous. On the other hand, we have not found any particular property which could differentiate the crystals for which the model is appropriate from those for which it is not.

The obvious conclusion is that the electronic cloud around the molecules is indeed distorted appreciably during the librational motion, and that further refinements of the model, based on theoretical considerations, will have to come from molecular orbital calculations, which may indicate in more detail the conditions under which the simple oriented gas model could be an acceptable zeroth order approximation to the problem of the Raman intensity of lattice modes.

*Fellow of the Consejo Nacional de Investigaciones Científicàs y Tècnicas.

[1]A. Fruhling, Ann. Phys. (Paris) 6, 40 (1951); J. Chem. Phys. 18, 1119 (1950).
[2]M. Suzuki, T. Yokyama, and M. Ito, Spectrochim. Acta A 24, 1091 (1968).
[3]M. Suzuki and M. Ito, Spectrochim. Acta A 25, 1017 (1969).
[4]M. Ito, M. Suzuki, and T. Yokoyama, "Excitons, Magnons, and Phonons," Proc. Int. Symp. Mol. Cryst., Beirut, 1967 (Cambridge U.P., London, 1968).
[5]G. R. Elliott and G. R. Leroi, J. Chem. Phys. 58, 1253 (1973).
[6]G. R. Elliott and G. E. Leroi, J. Chem. Phys. 59, 1217

(1973).
[7]D. E. Williams, J. Chem. Phys. 45, 3770 (1966).
[8]See, for instance, D. A. Dows, Rend. Sc. Int. Fis. "Enrico Fermi" 55 (1972); H. Bonadeo and E. D'Alessio, Rend. Sc. Int. Fis. "Enrico Fermi" 55 (1972).
[9]A. I. Kitaigorodskii, *Organic Chemical Crystallography* (Consultants Bureau, New York, 1961).
[10]G. Taddei, H. Bonadeo, M. P. Marzocchi, and S. Califano, J. Chem. Phys. 58, 966 (1973).
[11]H. Bonadeo and E. D'Alessio, Chem. Phys. Lett. 19, 117 (1973).
[12]H. Bonadeo, M. P. Marzocchi, E. Castellucci, and S. Califano, J. Chem. Phys. 57, 4299 (1972).
[13]D. E. Muller, T. Inoue, R. H. Larkin, and H. D. Stidham, Spectrochim. Acta A 27, 405 (1971).
[14]D. Swanson, L. C. Brunel, and D. A. Dows, J. Chem. Phys. (in press).
[15]E. A. D'Alessio and H. Bonadeo, Chem. Phys. Lett. 22, 559 (1973).
[16]J. B. Bates, D. M. Thomas, A. Bandy, and E. R. Lippincott, Spectrochim. Acta A 27, 637 (1971).
[17]E. Burgos, E. D'Alessio, and H. Bonadeo, (to be published).
[18]R. W. G. Wyckoff, *Crystal Structures, Vol. 6, The Structure of Benzene Derivatives* (Interscience, New York, 1969).
[19]C. L. Cheng, D. S. N. Murthy, and G. L. D. Ritchie, Aust. J. Chem. 25, 1301 (1972).
[20]M. Ghelfenstein and H. Szwarc, Mol. Cryst. Liq. Cryst. 14, 283 (1971).
[21]C. Dean, M. Pollack, B. M. Craven, and G. A. Jeffrey, Acta Crystallogr. 11, 710 (1968).
[22]D. A. Dows, L. Hsu, S. S. Mitra, O. Brafman, M. Hayek, W. B. Daniels, and R. K. Crawford, Chem. Phys. Lett. 22, 595 (1973).
[23]D. W. J. Cruickshank, Acta Crystallogr. 10, 504 (1957).
[24]D. W. J. Cruickshank, Acta Crystallogr. 9, 915 (1956).
[25]A. Hargreaves and H. Rizvi, Acta Crystallogr. 15, 365 (1962). J. Trotter, Acta Crystallogr. 14, 1135 (1961).
[26]R. J. W. LeFevre and D. S. N. Murthy, Aust. J. Chem. 21, 1903 (1968).
[27]H. A. Stuart and V. Schiessl, Ann. Phys. 2, 321 (1948).
[28]E. Manghi, C. A. de Caroni, M. R. de Benyacar, and M. J. de Abeledo, Acta Crystallogr. 23, 205 (1967).